

Artificial two-dimensional Mott insulating superstructures with a large Mott gap:
Theoretical Part
(Dated: April 7, 2021)

To have a better understanding of the experimental observations, we construct single-band Hubbard model with renormalized hopping coefficients to describe these systems and calculate the local density of states by using cluster perturbation theory (CPT)^{1,2}.

For the $(3\sqrt{7} \times 3\sqrt{7})R19.1^\circ$ surface (referred to as Phase 1 in the following), the corresponding proposed atomic structural is shown in Fig. 1(g). The unit cell contains twenty-three sites while three of them are somewhat isolated, i.e., the three blue circles are separated from the others. Considering that the hopping amplitude is inversely proportional to the square of the distance, it is reasonable to neglect the three isolated sites in a simplified model. We only include these hopping terms shown in Fig. 2 and the resulting Hamiltonian takes the following form:

$$H = \sum_{i,j,\sigma} t_{ij} (c_{i\sigma}^\dagger c_{j\sigma} + \text{H.c.}) + U \sum_i n_{i\uparrow} n_{i\downarrow} \quad (1)$$

where t_{ij} is the effective hopping amplitude and U the effective on-site Coulomb repulsion. In Fig. 2, the red points correspond to the center brightest spots in Fig. 1(d), and the blue points correspond to the surrounding less bright spots in Fig. 1(d). The hopping amplitudes between the center red point and the surrounding blue points are taken to be t_0 , and the hopping amplitudes between these adjacent blue points are t_1 . Since the atoms corresponding to the brightest spots in the center are not in the same atomic layer as the atoms corresponding to the less bright spots around (see Fig. 1(d)), t_0 should be less than t_1 . Here, we take $t_0 = -0.5$ and $t_1 = -1.0$.

For this model Hamiltonian, we first consider the non-interacting case (*i.e.*, $U = 0$) which can be diagonalized exactly. The averaged DOS and representative LDOS are shown in Fig. 3. It can be seen from the averaged DOS that the system has an energy gap of $\sim 0.3t_1$. However, the LDOS varies from site to site. For instance, the LDOS of the site labeled as “0” is quite different from the sites labeled as “1” and “3”. Especially, the energy gap at the zeroth site is $\sim 3.4t_1$, and yet that at other sites is $\sim 0.3t_1$. This inhomogeneous LDOS is obviously contradictory to the experimental uniform insulating gap. We further include on-site Coulomb repulsion and use CPT to calculate the LDOS. The evolution of the averaged DOS with U is shown in Fig. 4. The energy gap becomes gradually decreased when taking into account of Hubbard- U and a transition from band insulator to metal is identified at $U \approx 3.0t_1$. As we further increase U , an energy gap is reopened, indicating a metal-insulator transition. The including of $U = 6t_1$ leads to a large energy gap of $\sim 2.32t_1$ which is comparable with the experimental energy gap of $\sim 2.5\text{eV}$ if we take $t_1 = -1\text{eV}$.

We further explored the corresponding LDOS and found that the energy gap is uniform at each lattice sites from 0 to 19 (see Fig. 5), which is consistent with the experimentally observed homogeneous dI/dV spectra. The agreement between the experimental observation and theoretical calculation indicates the Mott origin of the large energy gap of $\sim 2.5\text{eV}$ for $(3\sqrt{7} \times 3\sqrt{7})R19.1^\circ$ surface.

For $(\sqrt{133} \times 4\sqrt{3})$ and (13×13) surfaces (referred to as Phase 2 and Phase 3 respectively), we similarly constructed the simplified model for theoretical calculations. Considering the substrate Si atoms form triangular lattice and the surface Sn atoms form well-ordered superstructures, we constructed Hubbard model on triangular lattice with renormalized hopping amplitudes between nearest neighbors to describe Phase 2 and Phase 3. The corresponding tight-binding model is shown in Fig. 6 and the red circle correspond to the extra point. For the non-interacting part, even though the unit cell contains odd number of electrons at half-filling, the band structure and the calculated DOS indicate their metallic state with non-vanishing DOS near E_F . We further calculate the DOS of the corresponding Hubbard model by using CPT and the evolution of DOS with Hubbard- U is shown in Fig. 7. With the inclusion of Hubbard- U , the system undergoes an metal-insulator transition at $U \approx 2t$. When we further increase U to $6t$ to be consistent with the value of Phase 1, the Mott gap is about $3.84t$. The calculated gap size of Phase 2 and Phase3 is larger than the gap size of Phase 1, which is qualitatively consistent the experimental observation. Due to the fact that the actual atomic arrangements are slightly deviated from the proposed model, we introduce randomness on the hopping amplitude to study the influence of deviations of the atomic positions, i.e., we set the hopping coefficients $t_{ij} = -A/r_{ij}$ where r_{ij} is the distance between the i -th and j -th lattice sites and A is random number. We can set the hopping amplitude to be in different range and the corresponding DOS are shown in Fig. ???. It can be seen from Fig. ???, random sampling of hopping amplitude A only has slightly influence on the resulting DOS which implies that the tiny influence of the deviation of the atomic positions. In addition, the theoretical calculations of the LDOS with $U = 6t$ at different lattice sites show the constant Mott gap, same as the uniform dI/dV spectra observed experimentally. The good agreements further confirm these two superstructures are also large-gap Mott insulators.

¹ C. Gros and R. Valentí, *Phys. Rev. B* **48**, 418 (1993).

² D. S  n  chal, D. Perez, and M. Pioro-Ladri  re, *Phys. Rev. Lett.* **84**, 522 (2000).

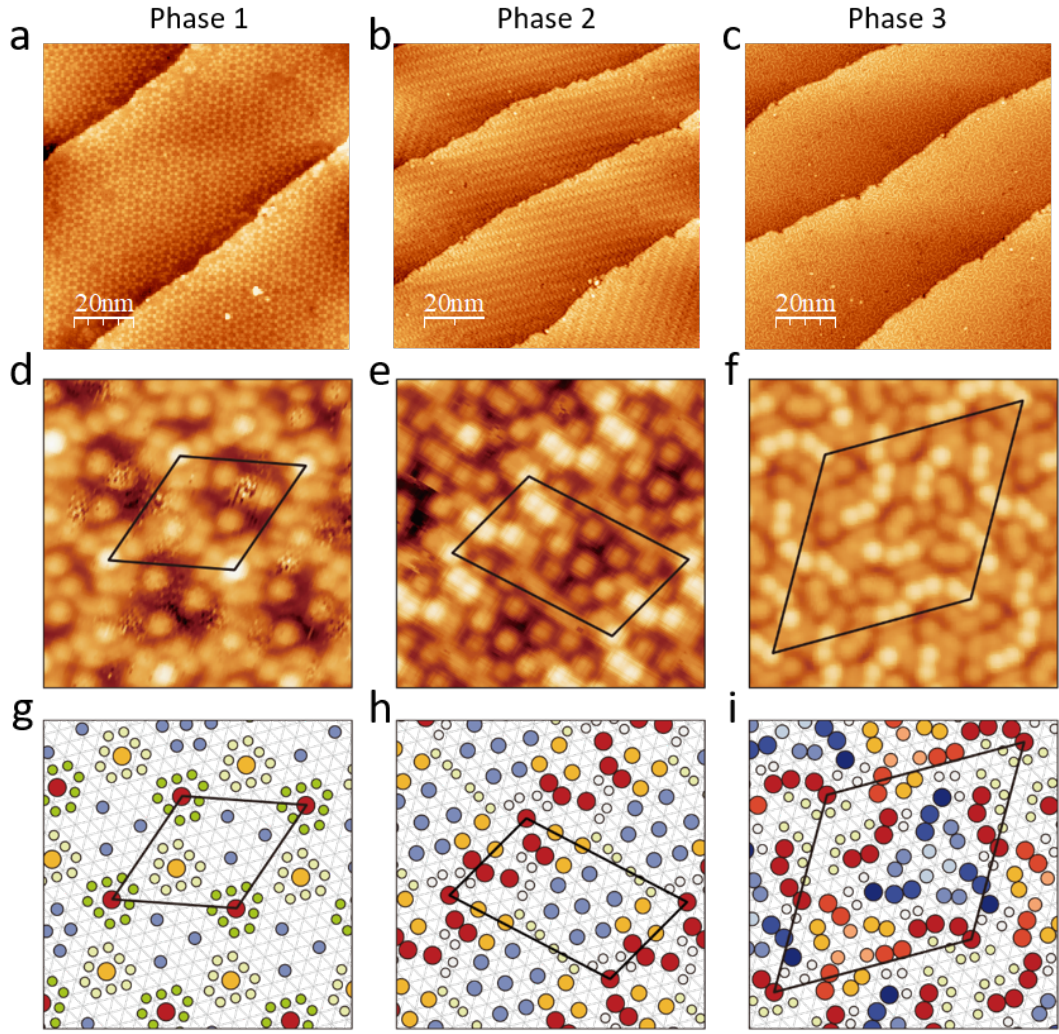


FIG. 1. (Color online) STM characterization of three new superstructures of Sn sub-monolayers on Si(111). (a)-(c) Large-scale STM image (size: $100 \times 100 \text{ nm}^2$) taken on $(3\sqrt{7} \times 3\sqrt{7})R19.1^\circ$, $(\sqrt{133} \times 4\sqrt{3})$, and (13×13) surfaces. They are taken at $U = +3.5V$, $U = -2V$, and $U = -2V$ ($I_t = 100pA$) respectively. (d)-(f) The atomically resolved STM images of them taken at $U = -2V$, $I_t = 200pA$. The surface unit cells of them are marked in black parallelogram. (g)-(i) The corresponding proposed atomic structural models. The marked surface unit cells in (g)-(i) are the same as these in (d)-(f).

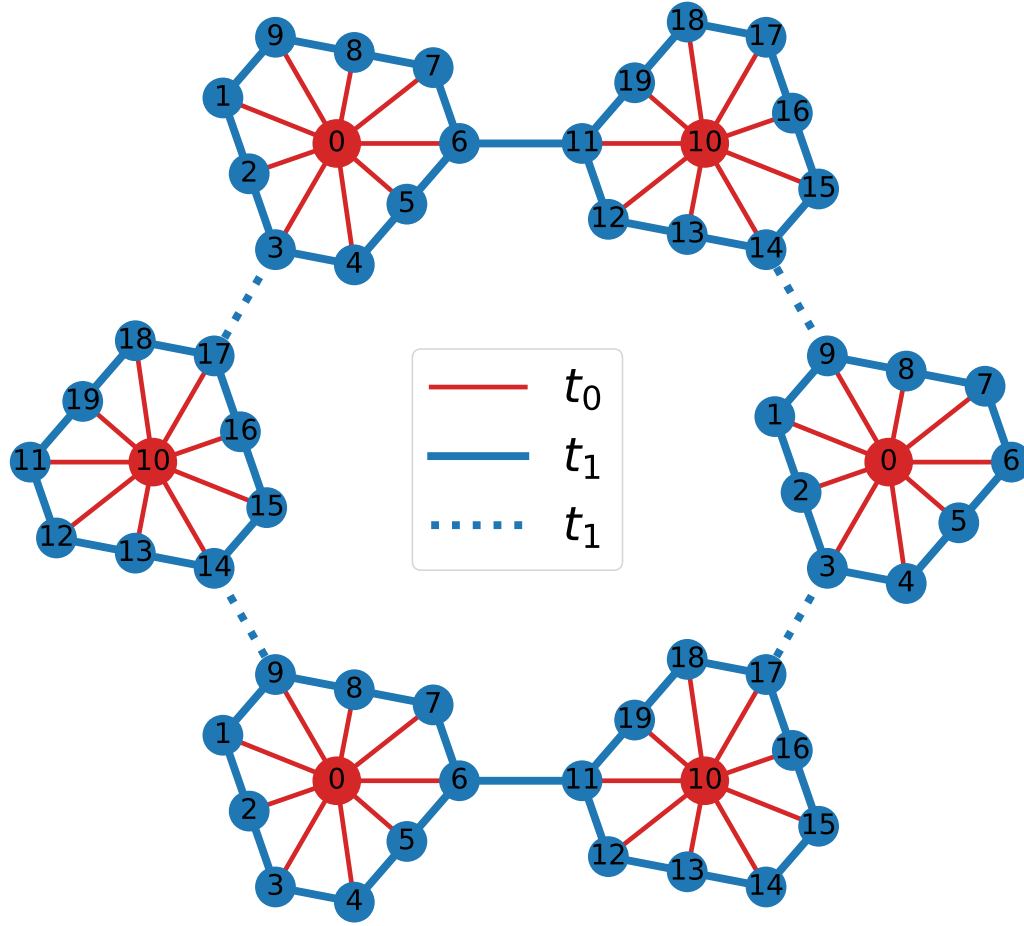


FIG. 2. (Color online) Demonstration of the hopping terms for Phase 1. The unit cell has twenty sites labeled from 0 to 19. The solid and dashed lines correspond to the hopping terms $t_{ij}(c_{i\sigma}^\dagger c_{j\sigma} + \text{H.c.})$.

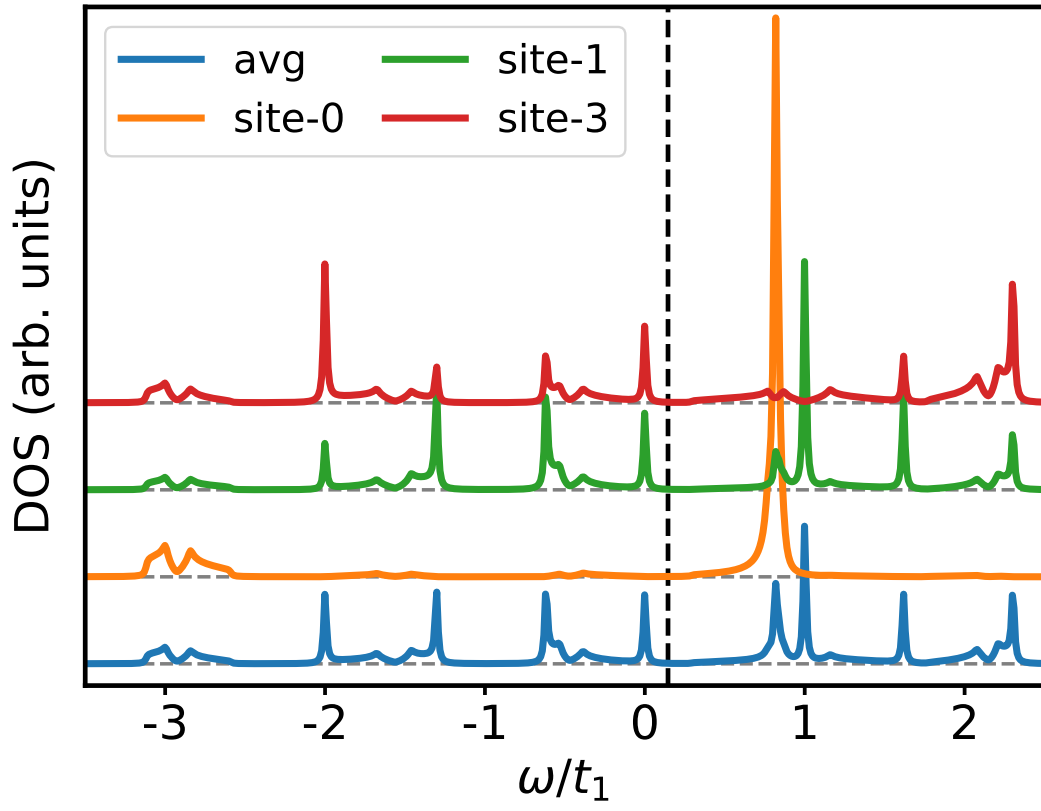


FIG. 3. (Color online) Local density of states calculated from the tight-binding model defined in Fig. 2. The blue line is the average of the LDOS over the twenty sites in a unit cell. LDOS for site $\{0, 10\}$, $\{3, 6, 9, 11, 14, 17\}$, $\{1, 2, 4, 5, 7, 8, 12, 13, 15, 16, 18, 19\}$ are the same. The gray dashed vertical line marks the Fermi energy E_F .

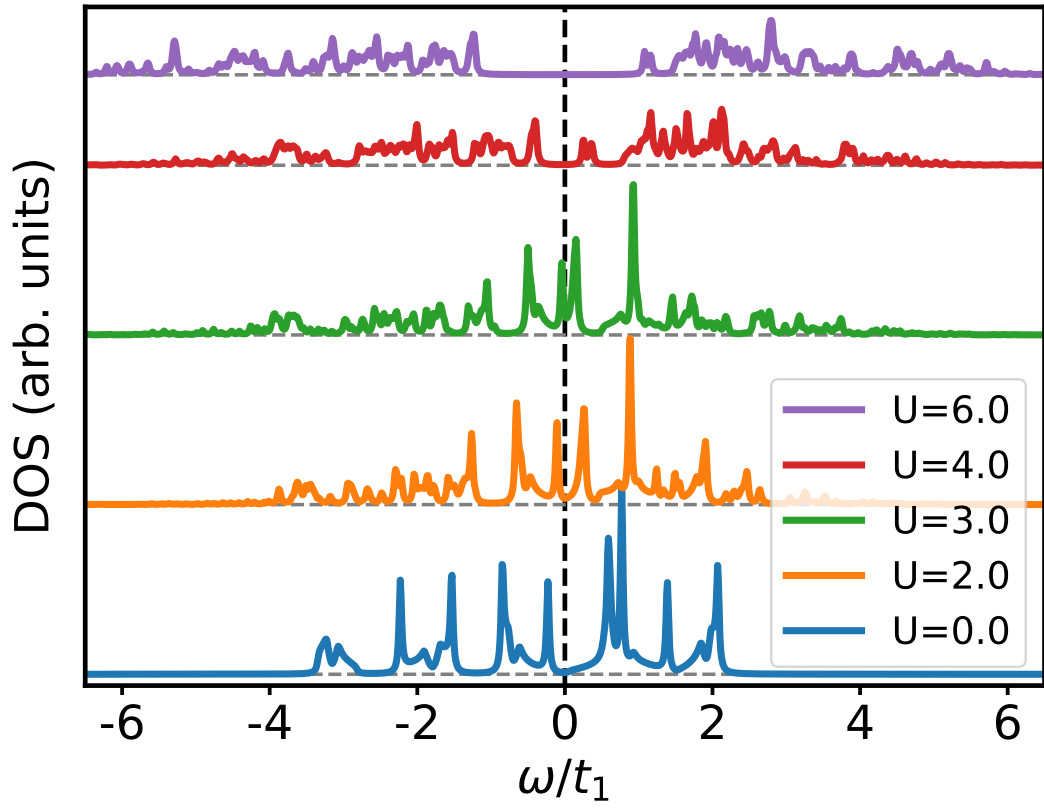


FIG. 4. (Color online) The evolution of averaged DOS with Hubbard- U . U is in the unit of t_1 .

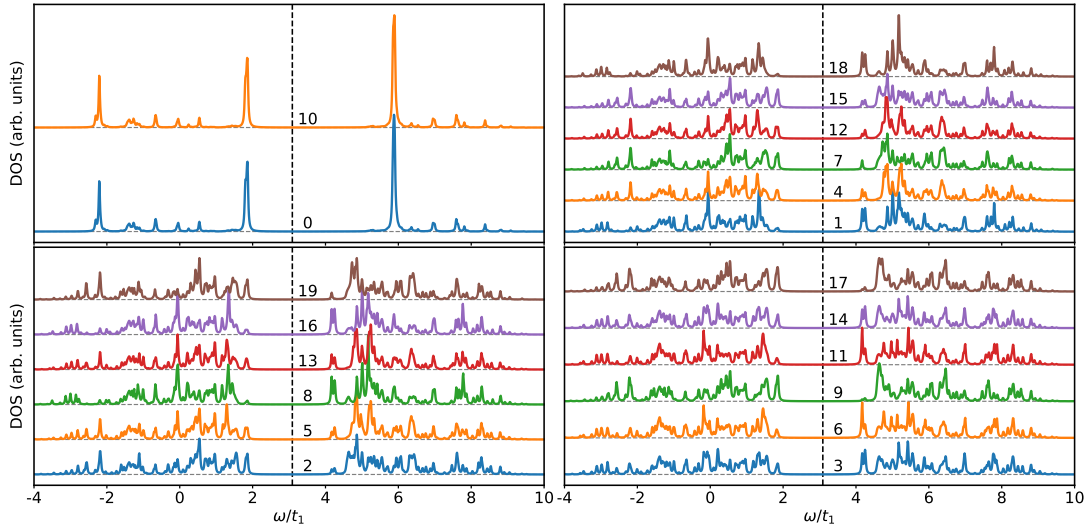


FIG. 5. Local density of states at $U = 6t_1$. The numbers above the curves correspond to the site indices shown in Fig. 2.

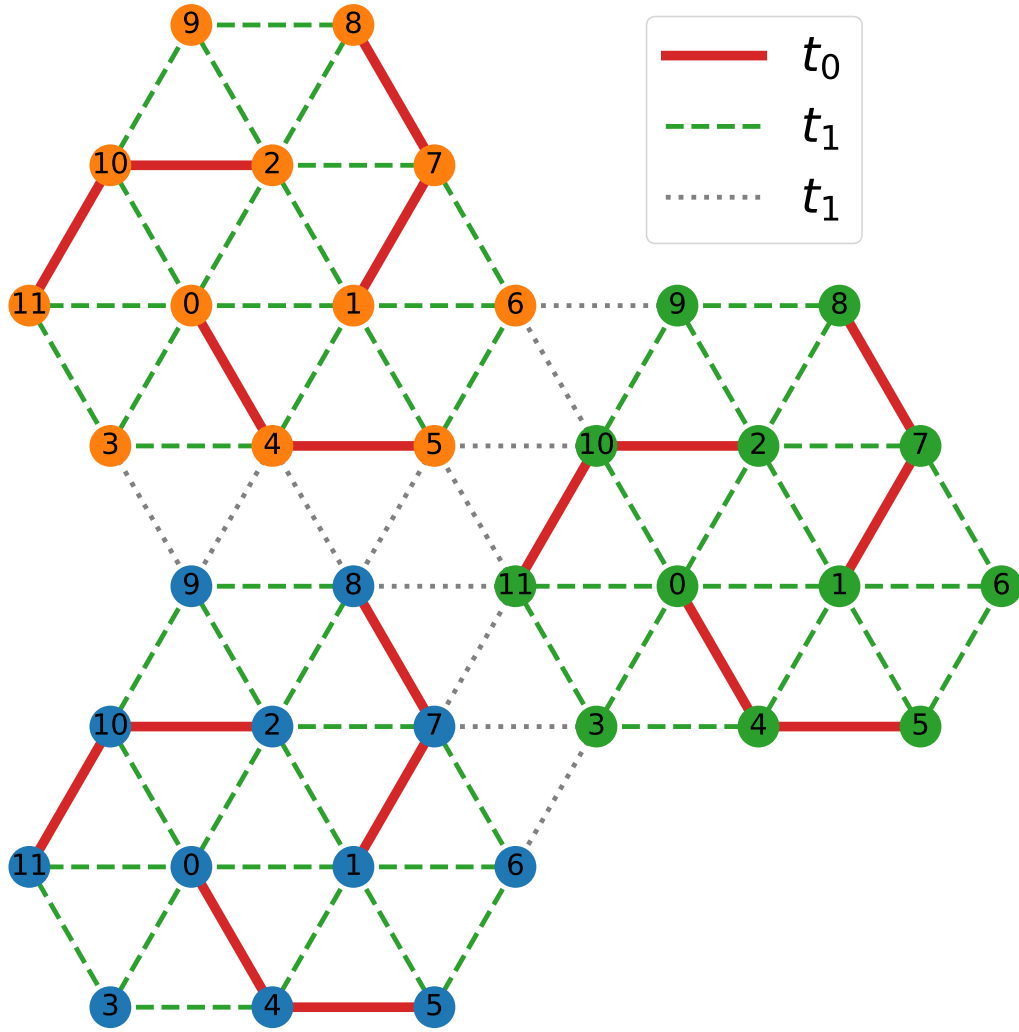


FIG. 6. (Color online) Demonstration of the tight-binding model for Phase 2 and Phase 3. The solid and dashed lines correspond to the hopping terms $t_{ij}(c_{i\sigma}^\dagger c_{j\sigma} + \text{H.c.})$, where $t_{ij} = -1/r_{ij}^2$ and r_{ij} is the distance from i -th to j -th site.

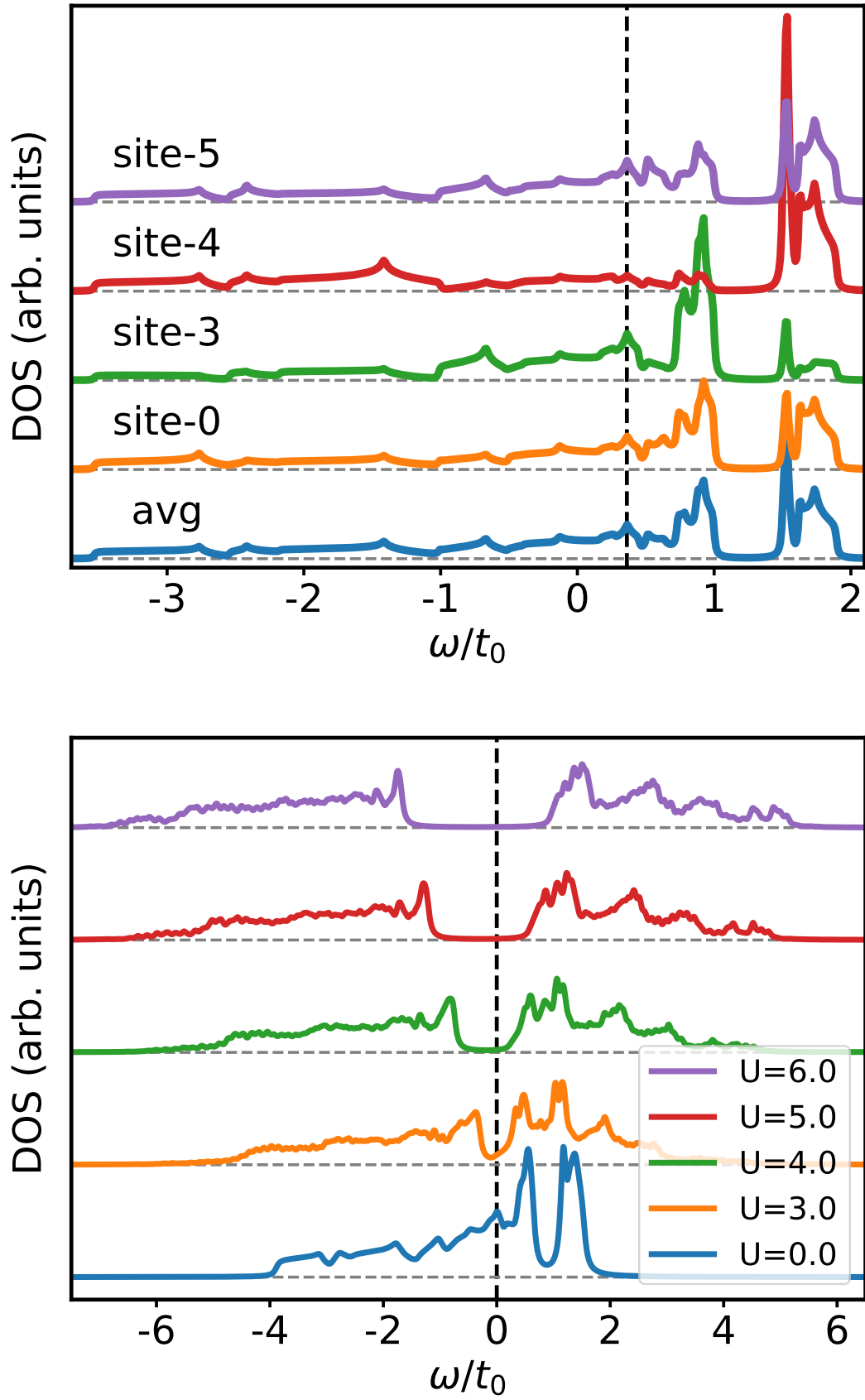


FIG. 7. (Color online) The evolution of averaged DOS with Hubbard- U .

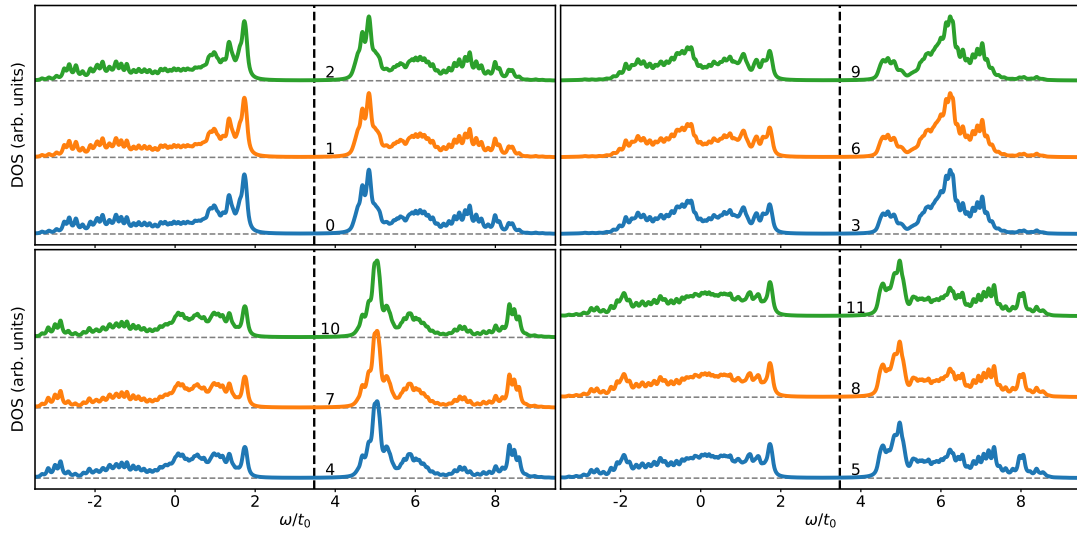


FIG. 8. (Color online) The evolution of averaged DOS with Hubbard- U .